ELSEVIER

Materials Science and Engineering A339 (2003) 73–80

MATERIALS SCIENCE & ENGINEERING A

www.elsevier.com/locate/msea

Transformations of grain boundaries due to disclination motion and emission of dislocation pairs

M.Yu. Gutkin, I.A. Ovid'ko *, N.V. Skiba

Institute of Problems of Mechanical Engineering, Russian Academy of Sciences, Bolshoj 61, Vas. Ostrov, St. Petersburg 199178, Russia

Received 12 October 2001; received in revised form 23 January 2002; accepted 14 February 2002

Abstract

A theoretical model is suggested which describes changes of grain boundary misorientation parameters in plastically deformed polycrystalline and nanocrystalline materials. In the framework of the model, the changes occur via grain boundary disclination motion associated with emission of dislocation pairs from grain boundaries into adjacent grain interiors. Energetic characteristics of the disclination motion in question are calculated.

Keywords: Grain boundaries; Dislocations; Disclinations; Polycrystalline materials; Nanocrystalline materials

1. Introduction

Transformations of grain boundaries often strongly influence both the structure and the properties of polycrystalline and nanocrystalline materials, e.g. [1–27]. Thus, plastic deformation processes in fine-grained polycrystals and nanocrystalline solids are associated with transformations of grain boundaries, that crucially affect the structure and mechanical characteristics of such solids [9–24,26]. In particular, changes of misorientation parameters of grain boundaries, that are capable of resulting in grain rotations, have been experimentally detected in polycrystalline and nanocrystalline materials under (super)plastic deformation (see, e.g. [9–12]). Recently, grain rotations have also been observed experimentally in thin films of gold under thermal treatment [25]. Changes of misorientation parameters of grain boundaries are related to their structural transformations giving rise to changes of the functional properties of polycrystalline and nanocrystalline materials. This causes interest to understanding the micromechanisms responsible for changes of boundary misorientation parameters. According to contemporary theoretical representations of grain boundaries, changes of their misorientation parameters occur via motion of grain boundary disclinations, defects of the rotational type [26–28]. In doing so, motion of grain boundary disclinations in plastically deformed materials is commonly treated as that associated with absorption of lattice dislocations (that are generated and move in grains under the action of mechanical load) by grain boundaries [12,26]. However, according to the general geometric theory of disclinations (see, e.g. [29,30]), their motion can also be associated with emission of dislocations. The main aim of this paper is to suggest a theoretical model, which describes changes of boundary misorientation parameters as those occurring via motion of grain boundary disclinations associated with emission of pairs of lattice dislocations from grain boundaries into adjacent grains.

2. Motion of grain boundary disclinations associated with emission of dislocation pairs. Key aspects

Following the theory of grain boundaries, two fragments of a grain boundary that are characterized by different values of tilt misorientation parameter are divided by a disclination, a line defect of the rotational type; see, e.g. [8,26–28]. More precisely, the line that

* Corresponding author: Tel.: +7-812-321-4764; fax: +7-812-321-4771.

E-mail address: ovidko@def.ipme.ru (I.A. Ovid'ko).

0921-5093/03/$ - see front matter
PII: S0921-5093(02)00107-7

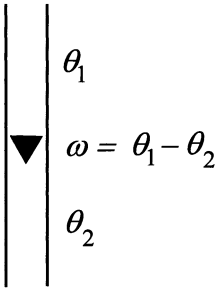

Fig. 1. Grain boundary disclination (black triangle) separates boundary fragments characterized by different values, θ_1 and θ_2 of tilt misorientation.

separates the two boundary fragments with tilt misorientation parameters θ_1 and θ_2, respectively, is described as the line of a grain boundary wedge disclination with strength $\omega = \theta_1 - \theta_2$ (Fig. 1). In the framework of the discussed representations, evolution (in time) of tilt misorientation along grain boundaries is treated as that related to the motion of grain boundary disclinations [26,27].

As it has been shown in the geometric theory of disclinations in solids, motion of disclinations is associated with either absorption or emission of dislocations [29,30]. Motion of grain boundary disclinations in plastically deformed polycrystalline and nanocrystalline materials is commonly described as that associated with absorption of lattice dislocations (that are generated and move in deformed grains under action of mechanical stresses) at grain boundaries [12,26]. This micromechanism, according to paper [12], is responsible for experimentally observed grain rotations in fine-grained materials during (super)plastic deformation. However, rotation of a grain as a whole occurs via a consequent transfer of a grain boundary disclination along all grain boundaries that surround the grain. The consequent motion of such a disclination requires processes of the dislocation absorption to be well ordered in space and time. In particular, dislocations with certain Burgers vectors have to reach a grain boundary in only vicinity of the disclination that moves along the boundary due to acts of absorption of these dislocations. This is in an evident contradiction with the fact that sources of lattice dislocations in plastically deformed materials are commonly distributed in a rather irregular way within a grain and, therefore, are not capable of providing the regular flow of dislocations to the disclination moving along a grain boundary. As a corollary, the representations [12] on motion of grain boundary disclinations associated with absorption of lattice dislocations during (super)plastic deformation are discussive.

In the situation with grain rotations in thin films of gold under thermal treatment [25], absorption of lattice dislocations by grain boundaries hardly plays an important role in changes of boundary misorientation parameters, because the dislocation density in grain interiors is too low to cause grain rotations. With this taken into account, we think that changes of boundary misorientation parameters in (super)plastically deformed and thermally treated materials occur mostly via motion of grain boundary disclinations associated with emission of dislocation pairs from grain boundaries into adjacent grain interiors.

Let us suggest and analyze a theoretical model that describes the process in question. In doing so, for definiteness and simplicity, we restrict our consideration to a bicrystal with a tilt boundary containing a wedge disclination of strength ω (Fig. 2). The configuration considered (Fig. 2) is assumed to be identical along axis z perpendicular to Fig. 2 plane. In the framework of the suggested model, an elementary act of transfer (by distance l) of a grain boundary disclination with strength ω is accompanied by emission of two lattice dislocations with Burgers vectors $\boldsymbol{b}_1$ and $\boldsymbol{b}_2$ from the grain boundary into the adjacent grains I and II, respectively (Fig. 2). The disclination with strength ω

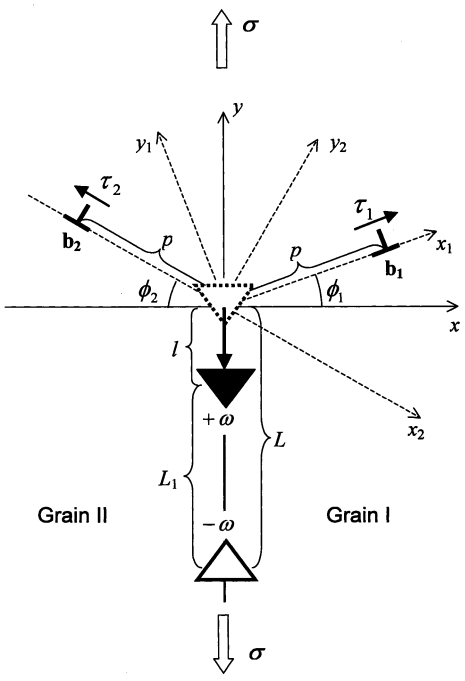

Fig. 2. Displacement of the wedge disclination (black triangle) with the strength ω from its initial position (dashed triangle) by the distance l is accompanied by the emission of two lattice dislocations with Burgers vectors $\boldsymbol{b}_1$ and $\boldsymbol{b}_2$. The ω-disclination moves along the grain boundary plane (which is perpendicular to the figure plane and intersects it along axis y) towards another disclination (white triangle) with the strength $-\omega$. The x-axis is normal to the grain boundary plane. The x_1y_1 and x_2y_2 coordinate systems are associated with the gliding planes of emitted dislocations. ϕ_1 and ϕ_2 are the angles between the normal to the grain boundary plane and the gliding planes of respectively the first and the second dislocations. τ_1 and τ_2 are the shear stresses acting along the gliding planes of the first and second dislocation, respectively. L and L_1 are the distances between the disclinations before and after displacement of the ω-disclination.

can be treated as that terminating a ragged wall of periodically spaced grain boundary dislocations with identical Burgers vectors $\boldsymbol{b}$ and spacing (period) l between the neighboring dislocations. This dislocation representation is relevant to both small- and large-angle boundaries with grain boundary dislocations having a 'large' crystal lattice Burgers vector $\boldsymbol{b}$ in the case of small-angle boundaries and a 'small' DSC-lattice Burgers vector $\boldsymbol{b}$ in the case of large-angle boundaries. With the spacing l between such dislocations assumed to be the distance of an elementary transfer of the disclination, Burgers vectors of the grain boundary dislocations and strength ω of the disclination obey the equations: $\boldsymbol{b}_1+\boldsymbol{b}_2=\boldsymbol{b}$, and $|\boldsymbol{b}|\approx l\omega$. From the former equation, one finds that the Burgers vector magnitude b is in the following relationship with the magnitudes, b_1 and b_2, of Burgers vectors of the emitted dislocations:

$$b=b_1\left(\cos\,\phi_1+\frac{b_2}{b_1}\cos\,\phi_2\right)=b_1\frac{\sin(\phi_1+\phi_2)}{\sin\,\phi_2}. \qquad (1)$$

where ϕ_1 and ϕ_2 are the angles between the normal to grain boundary plane and the gliding planes of the, respectively, first and second emitted lattice dislocations (Fig. 2). Notice that $b<b_1$, b_2 in the case of large-angle boundaries (containing dislocations with DSC-lattice Burgers vectors).

The consequent emission of lattice dislocation pairs (Fig. 2) causes change of boundary mis-orientation along large fragments of grain boundary plane. This process is capable of giving rise to the rotation of a grain as a whole in a plastically deformed nanocrystalline or polycrystalline material.

The suggested model (Fig. 2) is approximate. In particular, we restrict our consideration to the z-independent situation with a disclination dipole at tilt boundary characterized by two macroscopic geometric parameters, the angles ϕ_1 and ϕ_2 (Fig. 2). However, tilt boundaries which are effectively described in terms of disclinations [26], represent the most widespread type of grain boundaries in real materials, in which case our model covers most real grain boundaries. The choice of the disclination dipole as a subject of our theoretical analysis (addressed the grain boundary disclination motion) in this paper is related to the two following aspects: (i) the long-range stress field of the moving disclination should be screened, and (ii) there is an experimental evidence (see reviews [19,26] and references therein) that disclinations form dipole, quadrupole and multipole configurations in real materials under high-strain deformation. In our model we have chosen the simplest way to screen the long-range stress field of the moving (first) disclination by using the simplest self-screened disclination configuration (disclination dipole) among others which are observed in real materials.

In our model, the disclination dipole consists of mobile (first) and immobile (second) disclinations (Fig. 2). As with the first disclination, the second disclination may also represent the discontinuity of misorientation across the grain boundary, or may be a triple junction disclination, etc. It may also be as mobile as the first disclination is. This will not change results of our model (see next sections), because we will analyze only the energetic possibility for an elemental displacement of the first disclination. It would hardly be expected that both the disclinations must make such elemental 'jumps' simultaneously. Therefore, we can treat one of them as 'mobile' while another one as 'immobile'.

Finally, it should be noted that grain rotation in plastically deformed nanocrystalline and polycrystalline materials is a highly non-equilibrium process which is naturally realized via formation and evolution of unstable ('non-equilibrium') defect configurations. The dipole of grain boundary disclinations (Fig. 2) emitting lattice dislocations is the simplest (unstable) configuration that carries the non-equilibrium grain rotation under high-strain deformation. A theoretical analysis of characteristics of the dipole will allow us to understand the key basic features of the disclination motion (accompanied by emission of dislocation pairs) as a process capable of causing the grain rotation.

To summarize, the first approximation model suggested in this section is convenient for a strict mathematical analysis (see below) and effective for understanding the key peculiarities of changes of grain boundary misorientation parameters in plastically deformed materials. In the next section, we will use the model to quantitatively characterize grain boundary disclination motion giving rise to evolution of boundary misorientation.

3. Energetic characteristics of disclination motion associated with emission of dislocation pairs

Let us consider energetic characteristics of the boundary disclination motion under discussion. In doing so, we will focus our consideration on a concrete configuration of defects, namely a grain boundary disclination with strength ω, which moves to another (immobile) grain boundary disclination with strength $-\omega$ (Fig. 2). The disclinations, in fact, compose a dipole, in which case their stress fields screen each other at the distances exceeding the dipole arm L, the distance between the disclinations. The grain boundary disclinations can be treated as the defects terminating the boundary dislocation wall of finite extent (Fig. 3), in which case an elementary transfer of the moving disclination occurs via the splitting of one grain boundary dislocation belonging to the wall into two lattice dislocations (Fig. 3). The motion of the disclina-

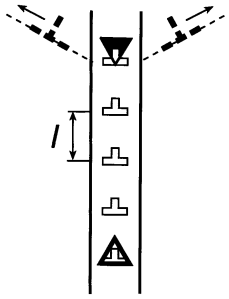

Fig. 3. Disclinations composing a dipole terminate a ragged wall of periodically (with period l) spaced grain boundary dislocations with either a crystal-lattice or DSC-lattice Burgers vector in respectively small- and large-angle boundaries. An elementary transfer of a moving disclination, shown in Fig. 2, is accompanied by the splitting of one of the grain boundary dislocations into the two lattice dislocations.

tion occurs under the action of external mechanical load which, in the framework of our model, causes uniaxial stress parallel with the grain boundary plane and promotes the motion of the emitted dislocations. Results and methods of our further theoretical analysis of the disclination configuration in question (Figs. 2 and 3) can directly be generalized to the situations with other disclination configurations and a more complicated stress state.

The elementary transfer of a grain boundary disclination by distance l, accompanied by emission of two lattice dislocations (Fig. 2), is energetically favorable, if the energy density (per unit disclination length) W_2 of the defect configuration resulted from the transfer is lower than the energy density W_1 of the pre-existent configuration (before the transfer): $\Delta W = W_2 - W_1 < 0$. To answer a question, if the transfer (Fig. 2) occurs as an energetically favorable process, let us calculate W_1 and W_2.

The pre-existent configuration represents a dipole of disclinations. Following [26], the energy density W_1 of the dipole of disclinations that terminate a ragged dislocation wall (Fig. 3) is given as:

$$W_1 = E_d = \frac{D\omega^2 L^2}{2}\left(\ln\frac{R}{L} + \frac{1}{2}\right) + NE_b^c, \tag{2}$$

where $D = G/2\pi(1-\nu)$, G denotes the shear modulus, ν the Poisson ratio, R the screening length for the dipole long-range stress field (which is of the dislocation type), N the number of the grain boundary dislocations composing the dislocation wall terminated by the disclination, and E_b^c the energy density that characterizes the dislocation core. This energy density is given as:

$$E_b^c = \frac{Db^2}{2}. \tag{3}$$

The energy density W_2 of the dipole configuration resulted from the elementary transfer (Fig. 2) can be written as follows:

$$W_2 = E_d' + E_{b_1} + E_{b_2} + E_d^{b_1} + E_d^{b_2} + E_{b_2}^{b_1} + E_\sigma^{b_1} + E_\sigma^{b_2} + (N-1)E_b^c. \tag{4}$$

Here E_d' denotes the energy density of the resultant disclination dipole characterized by dipole arm $L_1 = L - l$; E_{b_1} (E_{b_2}) proper energy density of the first (second) emitted dislocation; $E_d^{b_1}$ ($E_d^{b_2}$) the energy density that characterizes elastic interaction between the first (second) emitted dislocation and the disclination dipole; $E_{b_2}^{b_1}$ the energy density that characterizes elastic interaction between the emitted dislocations; and $E_\sigma^{b_1}$ ($E_\sigma^{b_2}$) the work of the external stress σ, spent to transfer of the first (second) dislocation to its position shown in Fig. 2.

The energy density E_d' of the disclination dipole with the arm L_1 is given by formula (Eq. (1)) with the substitution of L for L_1. The proper energy densities of the dislocations read [31]:

$$E_{b_i} = \frac{Db_i^2}{2}\left(\ln\frac{R}{r_0} + 1\right), \tag{5}$$

where $i = 1, 2$, and r_0 is the dislocation core radius (which is assumed to be the same for both dislocations under consideration).

After some algebra (see Appendices A, B and C), we find the following formulae for the energy densities $E_d^{b_i}$, $E_{b_2}^{b_1}$, and $E_\sigma^{b_i}$:

$$E_d^{b_i} = \frac{1}{2} D\omega b_i \cos\phi_i \left(L \ln\frac{R^2 + L^2 + 2RL\sin\phi_i}{p^2 + L^2 + 2pL\sin\phi_i} - l\ln\frac{R^2 + l^2 + 2Rl\sin\phi_i}{p^2 + l^2 + 2pl\sin\phi_i}\right), \tag{6}$$

$$E_{b_2}^{b_1} = Db_1b_2\left(\frac{1}{2}\cos(\phi_1+\phi_2) \times\ln\left[\frac{p^2 + R^2 + 2pR\cos(\phi_1+\phi_2)}{2ep^2[1+\cos(\phi_1+\phi_2)]}\right]\right) + Db_1b_2\left(\frac{1}{2} - \frac{pR\sin^2(\phi_1+\phi_2)}{p^2 + R^2 + 2pR\cos(\phi_1+\phi_2)}\right), \tag{7}$$

$$E_\sigma^{b_i} = -b_i p\sigma\frac{\sin 2\phi_i}{2}, \tag{8}$$

where σ is the external normal stress (Fig. 2). With formulae (Eqs. (1)–(8)), we find the difference ΔW between the energy densities of the defect configuration resulted from the elementary transfer of the grain boundary disclination and the pre-existent defect configuration (see Fig. 2). It is as follows:

$$\Delta W = \frac{Db_1^2}{2}\left(\left(1 + \frac{b_2^2}{b_1^2}\right)\left(\ln\frac{R}{r_0} + 1\right) - \frac{b^2}{b_1^2} + \frac{\omega^2 L_1^2}{b_1^2}\left[\ln\frac{R}{L_1} + \frac{1}{2} - \frac{L^2}{L_1^2}\left(\ln\frac{R}{L} + \frac{1}{2}\right)\right]\right)$$

$$-\frac{1}{2}\sigma p(b_1 \sin 2\phi_1 + b_2 \sin 2\phi_2)$$
$$+\frac{1}{2}D\omega b_1 \cos\phi_1\left(L\ln\frac{R^2+L^2+2RL\sin\phi_1}{p^2+L^2+2pL\sin\phi_1}\right.$$
$$\left.-l\ln\frac{R^2+l^2+2Rl\sin\phi_1}{p^2+l^2+2pl\sin\phi_1}\right)$$
$$+\frac{1}{2}D\omega b_2 \cos\phi_2\left(L\ln\frac{R^2+L^2+2RL\sin\phi_2}{p^2+L^2+2pL\sin\phi_2}\right.$$
$$\left.-l\ln\frac{R^2+l^2+2Rl\sin\phi_2}{p^2+l^2+2pl\sin\phi_2}\right)$$
$$+Db_1b_2\left(\frac{1}{2}\cos(\phi_1+\phi_2)\right.$$
$$\left.\times\ln\left[\frac{p^2+R^2+2pR\cos(\phi_1+\phi_2)}{2ep^2[1+\cos(\phi_1+\phi_2)]}\right]\right)$$
$$+Db_1b_2\left(\frac{1}{2}-\frac{pR\sin^2(\phi_1+\phi_2)}{p^2+R^2+2pR\cos(\phi_1+\phi_2)}\right), \quad (9)$$

where e is the base of the natural logarithm.

4. Results

Let us present results of our model as numerically calculated dependences (given by Eq. (9)) of ΔW on parameters, ϕ_1, ϕ_2, σ, R, p, and L, of the system under consideration. Thus, the dependences $\Delta W(p)$ are shown in Fig. 4, for various values of characteristic angles ϕ_1 and ϕ_2 related to the crystallography of the adjacent grains. These dependences, given by formula (Eq. (9)), indicate that angles ϕ_1 and ϕ_2 crucially influence elementary transfer of a grain boundary disclination (Fig. 2). In fact, the disclination transfer is energetically facilitated at low angles and hampered with rising ϕ_1 and ϕ_2. Thus, the disclination transfer is energetically unfavorable at high values (tentatively $>50^\circ$) of ϕ_1 and ϕ_2; there is an energetic barrier for motion of the emitted lattice dislocations (see Fig. 4). In the range of ϕ_1 and ϕ_2 from 0° to tentatively 20°, the dislocation motion has a barrier-less character with $\Delta W(<0)$ decreasing with rising the dislocation path p. In the range of ϕ_1 and ϕ_2 from tentatively 20 to 50°, the disclination transfer is either favorable or unfavorable, depending on other parameters (L, ω, σ) of the system. In this situation, the characteristic energy difference $\Delta W(p=b)$ at the starting point of the dislocation motion is highly sensitive to both the distance L between the disclinations and their strength magnitude ω (see Figs. 5 and 6) (in general, the disclination dipole arm L may be in the order of grain size or smaller. The former situation occurs when the dipole consists of triple junction disclinations. If one (mobile) disclination moves along a grain boundary towards another (immobile) triple junction disclination, the distance L between them is smaller than the grain size. This is why we have calculated $\Delta W(p)$ with p rising up to $4L$.) At the same time, $\Delta W(p=b)$ weakly depends on the external stress σ (see Fig. 7). The influence of the stress σ on the characteristic energy difference $\Delta W(p)$ increases with rising the dislocation path p at some intermediate values (close to 45°) of angles ϕ_1 and ϕ_2. The energy difference $\Delta W(p)$ at low values of angles ϕ_1 and ϕ_2 is weakly sensitive to σ, as is shown in Fig. 8. As the value of σ does not strongly influence the characteristic energy difference $\Delta W(p)$, a difference in the orientations of the external uniaxial stress also does not play any significant role in the process considered. One can make a similar conclusion with respect to more complicated stress state.

To summarize, $\Delta W<0$, i.e. the disclination motion (Fig. 2) is an energetically favorable process in rather

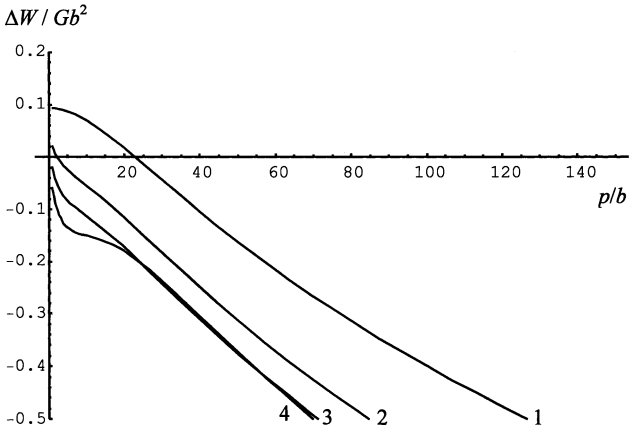

Fig. 4. Dependence of ΔW on the distance p moved by each of the emitted lattice dislocations, for $L=30b$, $\sigma=10^{-3}G$, $R=10^5b$, $\omega=0.1$, and the following values of the characteristic angles: $\phi_1=\phi_2=45^\circ$ (curve 1), $\phi_1=30^\circ$ and $\phi_2=40^\circ$ (curve 2), $\phi_1=20^\circ$ and $\phi_2=30^\circ$ (curve 3), $\phi_1=\phi_2=2^\circ$ (curve 4).

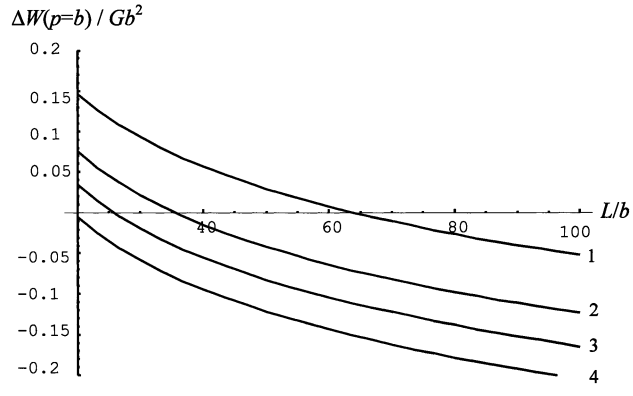

Fig. 5. Dependence of ΔW on the distance L between grain boundary disclinations at the initial stage of the dislocation emission (at $p=b$), for $\sigma=10^{-3}G$, $R=10^5b$, $\omega=0.1$, and the following values of the characteristic angles: $\phi_1=\phi_2=45^\circ$ (curve 1), $\phi_1=30^\circ$ and $\phi_2=40^\circ$ (curve 2), $\phi_1=20^\circ$ and $\phi=30^\circ$ (curve 3), $\phi_1=\phi_2=2^\circ$ (curve 4).

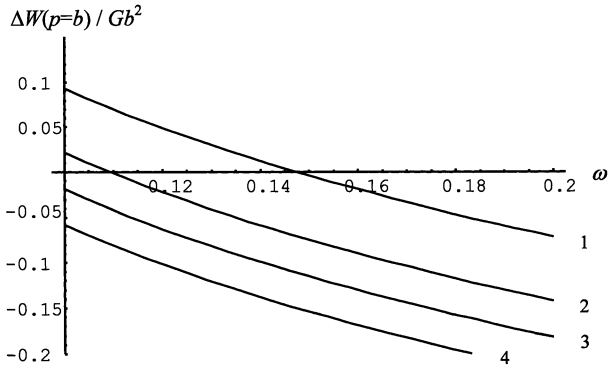

Fig. 6. Dependence of ΔW on the disclination strength ω at the initial stage of the dislocation emission (at $p = b$), for $\sigma = 10^{-3}G$, $R = 10^5 b$, $L = 30b$, and the following values of the characteristic angles: $\phi_1 = \phi_2 = 45^\circ$ (curve 1), $\phi_1 = 30^\circ$ and $\phi_2 = 40^\circ$ (curve 2), $\phi_1 = 20^\circ$ and $\phi_2 = 30^\circ$ (curve 3), $\phi_1 = \phi_2 = 2^\circ$ (curve 4).

wide ranges of parameters that characterize the defect configuration under consideration. Formula (Eq. (9)) that describes the energetic characteristics of the disclination motion towards a neighboring disclination (Fig. 2) can be directly generalized to disclination configurations of other types.

5. Concluding remarks

In this paper, it has been theoretically revealed that changes of misorientation parameters of grain boundaries can effectively occur via grain boundary disclination motion associated with emission of dislocation pairs into adjacent grains (Fig. 2). Our theoretical analysis of energetic characteristics of a grain boundary disclination which moves emitting dislocation pairs has indicated that the disclination motion in question is energetically favorable in rather wide ranges of parameters of the system. In contrast to the previously considered [12,26] situation with disclination motion associated with (ordered in space and time) absorption of dislocations by grain boundaries, the disclination motion associated with emission of dislocation pairs does not require any correlated flux of dislocations from grain interiors to grain boundaries. The suggested micromechanism for the disclination motion (Fig. 2) can be responsible for experimentally observed [9–11,25] rotations of grains in fine-grained materials under (super)plastic deformation and thermal treatment.

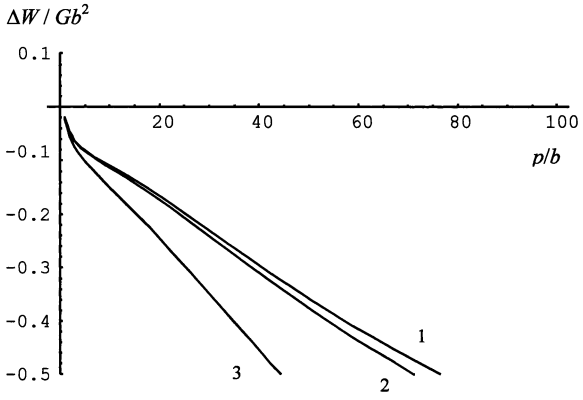

Fig. 7. Dependence of ΔW on the distance p moved by the emitted dislocations, for $\phi_1 = 30^\circ$ and $\phi_2 = 40^\circ$, $R = 10^5 b$, $L = 30b$, $\omega = 0.1$, and the following values of the applied stress $\sigma/G = 10^{-4}$, 10^{-3} and 10^{-2} (curves 1, 2 and 3, respectively).

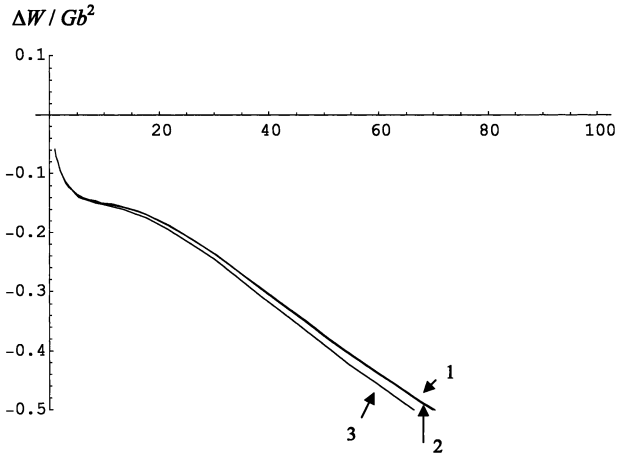

Fig. 8. Dependence of ΔW on the distance p moved by emitted dislocations, for $\phi_1 = \phi_2 = 2^\circ$, $R = 10^5 b$, $L = 30b$, $\omega = 0.1$, and the following values of the applied stress $\sigma/G = 10^{-4}$, 10^{-3} and 10^{-2} (curves 1, 2 and 3, respectively).

The results and methods of our model will serve as a basis for further theoretical and experimental examinations of transformations of grain boundaries and emission of lattice dislocations by grain boundaries in fine-grained polycrystalline and nanocrystalline materials. In particular, the motion of dipoles of grain boundary disclinations, associated with emission of dislocation pairs, is capable of effectively contributing to plastic deformation in nano crystalline materials where the density of grain boundary disclinations is expected to be very high. A theoretical analysis of the role of grain boundary disclinations and their dipoles in the deformation behavior of nanocrystalline materials will be the subject of further investigations of the authors.

Acknowledgements

This work was supported, in part, by the Office of US Naval Research (grant N00014-01-1-1020), the Russian Foundation of Basic Research (grants 01-02-16853 and 000-01-00482), INTAS (grant 99-01216), the Russian Research Council 'Physics of Solid-State Nanostructures' (grant 97-3006) and the Volkswagen Foundation (research project 05019225).

Appendix A

Let us calculate the energy density $E_{\mathrm{d}}^{b_1}$ that characterizes the elastic interaction between the first emitted dislocation and the disclination dipole (Fig. 2). Following [32], it can be calculated as the work spent to transfer the dislocation from infinitely distant point to its final position (shown in Fig. 2) in the shear stress τ_d created by the disclination dipole. That is, we have:

$$E_d^{b_1} = b_1 \int_p^{\infty} \tau_d(x_1, y_1 = 0)\mathrm{d}x_1. \tag{A.1}$$

To calculate integral figuring on the r.h.s. of Eq. (A.1), let us find formula for the disclination-dipole-induced shear stress τ_d that acts in the slip plane of the first emitted dislocation with Burgers vector $\boldsymbol{b}_1$. The stress τ_d can be expressed via components of the disclination-dipole-induced stress tensor σ_{ik} (written in the coordinate system shown in Fig. 2) as follows:

$$\begin{aligned}\tau_d = {} & \sigma_{xx}\alpha_1\alpha_2 + \sigma_{yy}\beta_1\beta_2 + \sigma_{zz}\gamma_1\gamma_2 + \sigma_{xy}(\alpha_1\beta_2 + \alpha_2\beta_1) \\ & + \sigma_{yz}(\beta_1\gamma_2 + \beta_2\gamma_1) + \sigma_{zx}(\gamma_1\alpha_2 + \gamma_2\alpha_1),\end{aligned} \tag{A.2}$$

where $\alpha_1 = \cos(x_1,\ x)$, $\beta_1 = \cos(x_1,\ y)$, $\gamma_1 = \cos(x_1,\ z)$, $\alpha_2 = \cos(y_1, x)$, $\beta_2 = \cos(y_1, y)$, and $\gamma_2 = \cos(y_1, z)$. Here the axes x_1, y_1 and z_1 are rotated by the angle ϕ_1 relative to the axes x, y and z of the coordinate system shown in Fig. 2. The components of stress tensor σ_{ik} are given by [26]:

$$\begin{aligned}\sigma_{xx} &= D\omega\left(\frac{(y+l)^2}{x^2+(y+l)^2} - \frac{(y+L)^2}{x^2+(y+L)^2} + \frac{1}{2}\ln\frac{x^2+(y+l)^2}{x^2+(y+L)^2}\right), \\ \sigma_{yy} &= D\omega\left(\frac{x^2}{x^2+(y+l)^2} - \frac{x^2}{x^2+(y+L)^2} + \frac{1}{2}\ln\frac{x^2+(y+l)^2}{x^2+(y+L)^2}\right), \\ \sigma_{zz} &= D\omega\nu\left(\ln\frac{x^2+(y+l)^2}{x^2+(y+L)^2}\right), \\ \sigma_{xy} &= D\omega\left(\frac{x(y+L)}{x^2+(y+L)^2} - \frac{x(y+l)}{x^2+(y+l)^2}\right), \\ \sigma_{xz} &= \sigma_{yz} = 0.\end{aligned} \tag{A.3}$$

Substitution of Eq. (A.3) into Eq. (A.2) results in

$$\begin{aligned}&\tau_d(x,y) \\ &= D\omega\left\{\left(\frac{x^2-(y+l)^2}{x^2+(y+l)^2} + \frac{(y+L)^2-x^2}{x^2+(y+L)^2}\right)\frac{\sin 2\phi_1}{2} \right. \\ &\left. + \left(\frac{x(y+L)}{x^2+(y+L)^2} - \frac{x(y+l)}{x^2+(y+l)^2}\right)\cos 2\phi_1\right\}\end{aligned} \tag{A.4}$$

This formula can be rewritten in the coordinate system (x_1, y_1, z_1) in the following form:

$$\begin{aligned}&\tau_d(x_1, y_1 = 0) \\ &= D\omega b_1 \\ &\times \frac{(l-L)x_1\cos\phi_1(-x_1[l\sin\phi_1 + x_1] + L[l\cos 2\phi_1 - x_1\sin\phi_1])}{(x_1^2 + L^2 + 2Lx_1\sin\phi_1)(x_1^2 + l^2 + 2lx_1\sin\phi_1)}.\end{aligned} \tag{A.5}$$

With Eq. (A.5) substituted to Eq. (A.1), we find the energy density $E_d^{b_1}$ as

$$\begin{aligned}E_d^{b_1} = \frac{1}{2}D\omega b_1\cos\phi_1\left(L\ln\frac{R^2+L^2+2RL\sin\phi_1}{p^2+L^2+2pL\sin\phi_1}\right. \\ \left. - l\ln\frac{R^2+l^2+2Rl\sin\phi_1}{p^2+l^2+2pl\sin\phi_1}\right).\end{aligned} \tag{A.6}$$

A similar formula for the energy density $E_d^{b_2}$ (that characterizes interaction between the second emitted dislocation and the dislocation dipole; see Fig. 2b) is derived in the same way. Both these expressions are represented by Eq. (6).

Appendix B

Let us calculate the energy density $E_{b_2}^{b_1}$ that characterizes the elastic interaction between the emitted dislocations. Following [32], it can be calculated as the work spent to transfer the first dislocation with Burgers vector $\boldsymbol{b}_1$ (shown in Fig. 2) in the shear stress created by the second dislocation with Burgers vector $\boldsymbol{b}_2$. In this situation, the energy reads

$$E_{b_2}^{b_1} = b_1 \int_p^{\infty} \tau_{b_2}(x_1, y_1 = 0)\mathrm{d}x_1. \tag{B.1}$$

Components of the second-dislocation-induced stress tensor, which contribute to the shear stress τ_{b2}, in coordinate system (x_2, y_2, z_2) (rotated by ϕ_2 relative to the coordinate system (x, y, z) shown in Fig. 2 are as follows [31]:

$$\sigma_{x_2x_2}^{b_2} = -Db_2y_2\frac{3(x_2+p)^2 + y_2^2}{[(x_2+p)^2 + y_2^2]^2},$$

$$\sigma_{y_2y_2}^{b_2} = Db_2y_2\frac{(x_2+p)^2 - y_2^2}{[(x_2+p)^2 + y_2^2]^2},$$

$$\sigma^{b_2}_{x_2y_2} = Db_2(x_2+p)\frac{(x_2+p)^2 - y_2^2}{[(x_2+p)^2 + y_2^2]^2}. \quad \text{(B.2)}$$

By analogy with calculation scheme considered in Appendix A, from Eq. (B.2) we find the following formula for the shear stress τ_{b_2} in the coordinate system (x_1,y_1,z_1):

$$\tau_{b_2}(x_1,y_1) = Db_2\frac{2p^3\cos 2(\phi_1+\phi_2) + p^2(5\cos(\phi_1+\phi_2) + \cos 3(\phi_1+\phi_2))x_1}{2(p^2 + 2p\cos(\phi_1+\phi_2)x_1 + x_1^2)^2} + Db_2 \times \frac{p(2+\cos 2(\phi_1+\phi_2))x_1^2 + \cos(\phi_1+\phi_2)x_1^3}{(p^2 - 2p\cos(\phi_1+\phi_2)x_1 + x_1^2)^2}. \quad \text{(B.3)}$$

Let us substitute Eq. (B.3) to Eq. (B.1) and integrate. As a result, we find Eq. (7) for the energy density $E^{b_1}_{b_2}$.

Appendix C

The work spent to transfer the first dislocation over the distance p under external-load-induced shear stress τ_1 is given by [31]:

$$E^{b_1}_{\sigma} = -b_1 p\tau_1, \quad \text{(C.1)}$$

where τ_1 yields from the geometry of the system as follows:

$$\tau_1 = \sigma_x\frac{\sin 2\phi_1}{2}. \quad \text{(C.2)}$$

From Eq. (C.1) and Eq. (C.2) we get

$$E^{b_1}_{\sigma} = -b_1 p\sigma_x\frac{\sin 2\phi_1}{2}. \quad \text{(C.3)}$$

The work $E^{b_2}_{\sigma}$ spent to transfer the second emitted dislocation under the action of external-load-induced shear stress acting in the dislocation gliding plane, is obtained by substitution of b_1 for b_2, and ϕ_1 for ϕ_2. Both the final expressions are represented by Eq. (8).

References

[1] A.P. Sutton, R.W. Balluffi, Interfaces in Crystalline Materials, Clarendon Press, Oxford, 1995.
[2] J.P. Hirth, Acta Mater. 48 (2000) 93.
[3] H. Gleiter, Mater. Sci. Eng. A 52 (1982) 91.
[4] L.G. Kornlelyuk, A.Yu. Lozovoi, I.M. Razumovskii, Philos. Mag. A 77 (1998) 465.
[5] M.Yu. Gutkin, I.A. Ovid'ko, Phys. Rev. B 63 (2001) 064515.
[6] M.Yu. Gutkin, I.A. Ovid'ko, Philos. Mag. A 70 (1994) 561.
[7] I.A. Ovid'ko, in: G.-M. Chow, I.A. Ovid'ko, T. Tsakalakos (Eds.), Nanostructured Films and Coatings, NATO Science Ser., Kluwer, Dordrecht, 2000, p. 231.
[8] S.V. Bobylev, I.A. Ovid'ko, A.G. Sheinerman, Phys. Rev. B 64 (2001) 224507.
[9] K.A. Padmanabhan, G.J. Davies, Superplasticity, Springer, Berlin, 1980.
[10] J. Pilling, N. Ridle, Superplasticity in Crystalline Solids, The Institute of Metals, London, 1989.
[11] M.G. Zelin, A.K. Mukherjee, Mater. Sci. Eng. A 208 (1996) 210.
[12] R.Z. Valiev, T.G. Langdon, Acta Metall. 41 (1993) 949.
[13] M. Mayo, D.C. Hague, D.-J. Chen, Mater. Sci. Eng. A 166 (1993) 145.
[14] M. Jain, T. Christman, Acta Metall. Mater. 42 (1994) 1901.
[15] R.S. Mishra, R.Z. Valiev, A.K. Mukherjee, Nanostruct. Mater. 9 (1997) 473.
[16] V.V. Astanin, O.A. Kaibyshev, S.N. Faizova, Scripta Metall. Mater. 25 (1991) 2663.
[17] H.S. Yang, M.G. Zelin, Scripta Metall. Mater. 26 (1992) 1707.
[18] M. Seefeldt, P. Van Houtte, Mater. Phys. Mech. 1 (2000) 133.
[19] M. Seefeldt, Rev. Adv. Mater. Sci. 2 (2001) 44.
[20] M.J. Mayo, Nanostruct. Mater. 9 (1997) 717.
[21] B. Baudelet, Scripta Metall. Mater. 27 (1992) 745.
[22] M.G. Zelin, R.Z. Valiev, M.V. Grabski, J.W. Wyrzykowski, H.S. Yang, A.K. Mukherjee, Mater. Sci. Eng. A 160 (1993) 215.
[23] M.G. Zelin, A.K. Mukherjee, Acta Metall. Mater. 43 (1995) 2359.
[24] M.G. Zelin, A.K. Mukherjee, J. Mater. Res. 10 (1995) 864.
[25] K.E. Harris, V.V. Singh, A.H. King, Acta Mater. 46 (1998) 2623.
[26] A.E. Romanov, V.V. Vladimirov, in: F.R.N. Nabarro (Ed.), Dislocations in Solids, vol. 9, North-Holland Publ, Amsterdam, 1992, p. 191.
[27] P. Müllner, W.-M. Kuschke, Scripta Mater. 36 (1997) 1451.
[28] K.N. Mikaelyan, I.A. Ovid'ko, A.E. Romanov, Mater. Sci. Eng. A 288 (2000) 61.
[29] W.F. Harris, L.E. Scriven, J. Appl. Phys. 42 (1971) 3309.
[30] R. de Wit, J. Appl. Phys. 42 (1971) 3304.
[31] J.P. Hirth, J. Lothe, Theory of Dislocations, Wiley, New York, 1982.
[32] T. Mura, in: H. Herman (Ed.), Advances in Material Research, vol. 3, Interscience, New York, 1968, p. 1.